Final Technical Report

Award No. DE-SC0008792

Indiana University

Project Title: Metal—Organic Surface Catalyst for Low-temperature Methane Oxidation: Bi-functional Union of Metal—Organic Complex and Chemically Complementary Surface

Principal Investigator (PI): Steven L. Tait

October 1, 2016

Report no. DE-IU-0008792

Reporting period: September 15, 2015 – September 14, 2016

DOE Program Office: US DOE Office of Science (SC) Basic Energy Sciences (BES)

Project Title: Metal—Organic Surface Catalyst for Low-temperature Methane Oxidation: Bi-functional Union of Metal—Organic Complex and Chemically Complementary Surface

Award No. DE-SC0008792

Steven L. Tait

Indiana University

Abstract

Stabilization and chemical control of transition metal centers is a critical problem in the advancement of heterogeneous catalysts to next-generation catalysts that exhibit high levels of selectivity, while maintaining strong activity and facile catalyst recycling. Supported metal nanoparticle catalysts typically suffer from having a wide range of metal sites with different coordination numbers and varying chemistry. This project is exploring new possibilities in catalysis by combining features of homogeneous catalysts with those of heterogeneous catalysts to develop new, bi-functional systems. The systems are more complex than traditional heterogeneous catalysts in that they utilize sequential active sites to accomplish the desired overall reaction. The interaction of metal—organic catalysts with surface supports and their interactions with reactants to enable the catalysis of critical reactions at lower temperatures are at the focus of this study.

Our work targets key fundamental chemistry problems. How do the metal—organic complexes interact with the surface? Can those metal center sites be tuned for selectivity and activity as they are in the homogeneous system by ligand design? What steps are necessary to enable a cooperative chemistry to occur and open opportunities for bi-functional catalyst systems? Study of these systems will develop the concept of bringing together the advantages of heterogeneous catalysis with those of homogeneous catalysis, and take this a step further by pursuing the objective of a bi-functional system.

The use of metal-organic complexes in surface catalysts is therefore of interest to create well-defined and highly regular single-site centers. While these are not likely to be stable in the high temperature environments (> 300 °C) typical of industrial heterogeneous catalysts, they could be applied in moderate temperature reactions (100-300 °C), made feasible by lowering reaction temperatures by better catalyst control. They also serve as easily tuned model systems for exploring the chemistry of single-site transition metals and tandem catalysts that could then be developed into a zeolite or other stable support structures.

In this final technical report, three major advances our described that further these goals. The first is a study demonstrating the ability to tune the oxidation state of V single-site centers on a surface by design of the surrounding ligand field. The synthesis of the single-site centers was developed in a previous reporting period of this project and this new advance shows a distinct new ability of the systems to have a designed oxidation state of the metal center. Second, we demonstrate metal complexation at surfaces using vibrational spectroscopy and also show a metal replacement reaction on Ag surfaces. Third, we demonstrate a surface-catalyzed dehydrocyclization reaction important for metal-organic catalyst design at surfaces.

Introduction

The energy challenges that face our country will only be resolved by new innovation to develop new technology, and to use existing technologies and run essential industries in more efficient ways. Catalysis research is a critical component of the solution portfolio to our energy challenges. This project will explore new possibilities in catalysis by combining features of homogeneous catalysts with those of heterogeneous catalysts to develop new, bi-functional systems. We have studied the interactions of metal—organic catalysts with surface supports and their interactions with reactants to enable the catalysis of critical reactions at lower temperatures. We have developed a bi-functional catalyst system, consisting of a metal—organic complex, similar to the complex used in the homogeneous systems, stabilized on metal surfaces.

We have applied a suite of analytical tools to characterize these systems. Scanning tunneling microscopy (STM) provides structural information. STM can provide a molecular level insight into the arrangement and assembly of the metal—organic complexes. X-ray photoelectron spectroscopy allows for quantitative assessment of the elemental composition of the systems, as well as detect changes in the chemical states of the elements in the system. High-resolution electron energy loss spectroscopy allows identification of bonds forming and breaking and is essential in examining reactions.

High selectivity in next-generation catalysts requires structural as well as chemical control of single-site metal centers at surfaces in order to maintain uniform and specific chemistry at all active sites. On-surface metal-ligand coordination is a promising strategy to achieve structurally and chemically well-defined metal centers [1], while also providing an opportunity for bi-functional character through intimate contact with a surface. A key challenge in the on-surface assembly of metal-ligand coordination networks is to develop a ligand library to access and program any one of a variety of metal oxidation states, which is important for tuning chemical selectivity in heterogeneous catalysis [2, 3]. Several prior examples of on-surface metal-ligand coordination involved diatomic elimination (*e.g.*, H_2), as in porphyrin [4, 5] and terephthalic acid [6] metalation with surface-supported elemental metal, such that the resultant complexed metals adopted a +2 oxidation state. In our prior studies of direct donation of electrons into a redox-active tetrazine [7] or ketone-functionalized phenanthroline [8] a +2 metal oxidation state was also achieved for platinum, chromium, and iron, and without diatomic elimination. This demonstrated on-surface redox chemistry to produce structurally uniform single site metal(2+) centers which are also uniform in oxidation state. Here, we report the implementation of redox non-innocent ligands to achieve the essential ability to change the metal oxidation state by rational molecular design of redox-active sub-units and thus achieve higher oxidation states than +2.

Typical metal nanoparticle catalysts have a variety of surface sites with different local coordination environments [9-13], which leads to the lower selectivity of the catalyst [14, 15]. On the other hand, metal-organic complexes commonly have single-site metal atom centers with specific coordination environments due to a well-defined ligand field [16-18], resulting in metal centers that have a uniform oxidation state and chemical reactivity. Significant progress has been made in developing thin film growth of metal organic frameworks (MOF) [19-22], as well as more fundamental studies of metal-organic coordination in 1D and 2D geometries in the first monolayer at surfaces [23-25]. There is growing interest in this class of materials, including exploration of on-surface metal-ligand redox reaction to form metal centers that are in intimate chemical contact with the underlying surface to take advantage of reverse spillover and other surface-assisted reaction pathways.

Description of Research Accomplishments

Here, we describe three key research advances in this funding period.

1. Two and Three Electron Oxidation of Single-site Vanadium Centers at Surfaces by Ligand Design

Text and figures in this section are adapted from D. Skomski, C. D. Tempas, B. J. Cook, A. V. Polezhaev, K. A. Smith, K. G. Caulton, and S. L. Tait, "Two and Three Electron Oxidation of Single-site Vanadium Centers at Surfaces by Ligand Design," *Journal of the American Chemical Society*, ***137***, *7898-7902* (2015).

We were interested in demonstrating a controlled variation in the ligand field to access a +2 or a +3 oxidation state in related metal species, while leaving the axial site of the metal unoccupied and thereby available for subsequent binding. Here, we present examples of the oxidation of metallic (*i.e.*, charge-neutral) vanadium to the +2 or +3 oxidation state by coordination to bis-pyridinyltetrazine or bis-pyrimidinyltetrazine, respectively, on the reconstructed Au(100) surface.

Tetrazines, which possess a low-lying π^* orbital due to their heavy sp^2 nitrogen loading, are known to act as an oxidant to an electron rich metal [26]. We previously illustrated the utility of bis-pyridinyltetrazine (**1**, Scheme 1) to ligate and oxidize Pt metal atoms to the +2 oxidation state on a gold surface [7]. Oxidation to the common Pt +4 oxidation state was not observed. To achieve higher oxidation states, we thus considered V, which has applications in heterogeneous catalysis [2, 27], including for selective alkane oxidation [28], and in homogeneous catalysis [29, 30] and is a stronger reducing agent than Pt. Also, V is known to be able to access a greater variety of oxidation states (-3 to +5) [31] although none of these have been previously characterized in an on-surface environment for metal-ligand systems; only various VO_x surfaces have been characterized in surface studies [32].

The experiments were conducted in a pristine ultra-high vacuum (UHV) system equipped with both scanning tunneling microscopy (STM) and X-ray photoelectron spectroscopy (XPS) STM imaging and XPS acquisition were conducted at room temperature. The reconstructed gold (100) single crystal surface was cleaned before each experiment by 3-4 cycles of argon ion sputtering, with the sample held at 200 °C, and thermal annealing to 550 °C. Under these conditions, the Au(100) surface spontaneously reconstructs to a quasi-hexagonal c(26x68) reconstruction [33, 34]. Bis-pyridinyltetrazine (**1**, 96%) was purchased from Sigma-Aldrich. Bis-pyrimidinyltetrazine (**2**) was synthesized by a coupling reaction between benzenediazonium salts and 1,3,5-triaminobenzene, followed by oxidative cyclization of the azo intermediate, in a procedure adapted from Kaim and Fees [35]. Vanadium (99.8% pure rod, Goodfellow) was vapor deposited using an electron beam evaporator.

XPS measurements of the V $2p_{3/2}$ photoelectron peak allow direct characterization of the core level electron binding energies, which will vary with the oxidation state of V and can thus be used to probe the effect of the redox reaction with ligands **1** or **2** on the V charge state. The V $2p_{3/2}$ BE for a sub-monolayer quantity of pure V (no ligand) on the reconstructed Au(100) surface (Fig. 1a; 512.7 eV) matches the value reported for bulk V metal (charge-neutral) (512.7 eV [36]) showing that final state effects in the V/Au surface environment are comparable those at the V surface, as expected [37]. Ligand **1** induces a 1.1 eV chemical shift of V 2*p* to higher BE (Fig. 1b, 513.8 eV), consistent with oxidation of V. This shift is comparable to that expected from comparison to V(II)-phthalocyanine on Ag(111) [38] or vanadium(II) oxide [32]. Ligand **2** induces a 1.9 eV chemical shift to higher BE (Fig. 1c, 514.7 eV) indicating still greater oxidation

than by **1**. Each of these data sets is fit well by a single component, indicating a quantitative yield of the on-surface oxidation of the V metal, *i.e.*, XPS does not resolve residual charge-neutral V. The V binding energy in **2**-V matches the +3 oxidation state in V(III)-N complexes, such as VN [39] and V-hydrazide [40] (514.4 – 515.0 eV). Since pyrimidinyl is an electron withdrawing group on the tetrazine (lowers the π^* energy) **2** is more easily reduced than **1**, and **2** will delocalize electrons from the tetrazine into both pyrimidinyl rings creating amide nitrogen atoms there (see Scheme 1). Consequently, the pyrimidinyl nitrogen atoms also become stronger donors in coordinate covalent bonds to the oxidized vanadium in the 1D polymer structure. The pyridinyl substituents in **1** are less effective electron acceptors than the pyrimidinyls in **2**; thus, the V 2*p* binding energy of **1**-V falls between the charge-neutral V metal and **2**-V and is assigned to the +2 chemical state [32, 41]. The model presented in Scheme 1 assumes that all charge is maintained in the 2D plane, but there is certainly some charge transfer to/from the surface and the induced charge in the metallic surface may play a significant role in stabilizing the polymer chains [42].

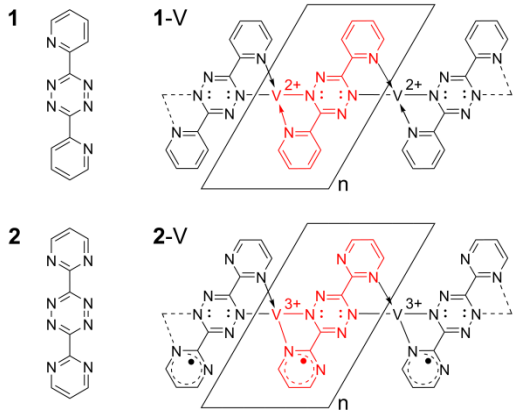

Scheme 1. Bis-pyridinyltetrazine (**1** or DPTZ) and bis-pyrimidinyltetrazine (**2**) ligands used in this study and the $(\mathbf{1}^{2-}\text{–}V^{2+})_n$ and $(\mathbf{2}^{3-}\text{–}V^{3+})_n$ polymers that result from their redox assembly on the Au(100) surface. One repeat unit is shown in red for each polymer.

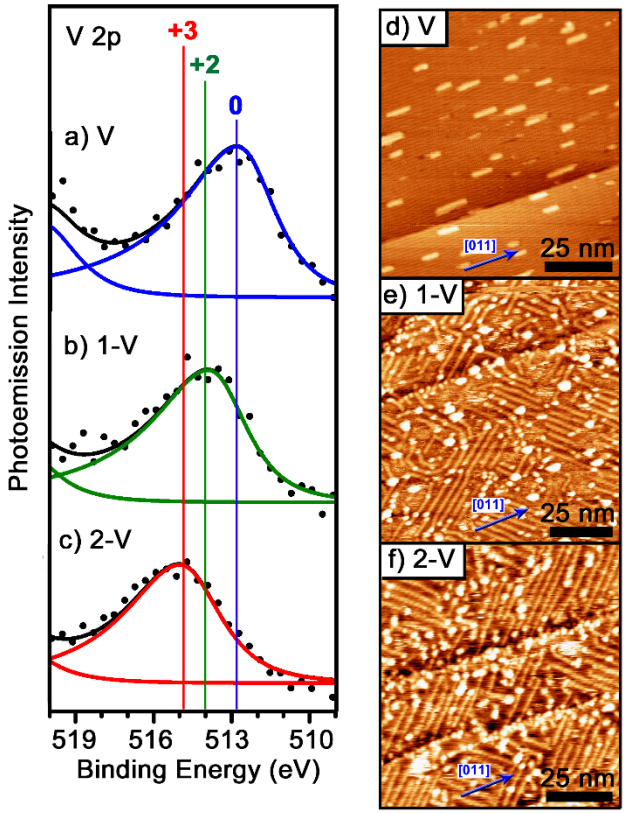

Figure 1. (a, b, c) Vanadium $2p_{3/2}$ XP spectra and (d, e, f) STM images for (a, d) V, (b, e) **1**-V, and (c, f) **2**-V on the reconstructed Au(100) surface after annealing at 170-200 °C. In each of **1**-V and **2**-V, the V:ligand ratio is 1 and the ligand was deposited first and V metal second with sub-monolayer quantities of each. (b) Oxidation of V by ligand **1** is evidenced by the 1.1 eV shift to higher binding energy, consistent with V(II)-phthalocyanine on Ag(111) [38] and V(II) oxide [32]. (c) Oxidation of V by ligand **2** is evidenced by the 1.9 eV shift to higher binding energy and referenced to V(III)-N complexes [39, 40]. (d) Wide-scan STM image of the V islands (bright nanoparticles) which are elongated along the rows of the Au reconstruction. (e, f) The metal-ligand chains are predominantly oriented at a 45° angle from the direction of the Au reconstruction. XPS analysis of the N 1*s* core levels of the ligands in the metal-ligand complexes shows a significant spectroscopic change, indicating an alteration in chemical state upon redox assembly and supporting the oxidation state analysis of the V.

The redox assembly occurs regardless of the deposition order of the metal and the ligand. Control experiments conducted with deposition of only V or with deposition of only ligand were conducted. In either case, no evidence for redox activity is observed unless both components are present. Further control studies that vary the relative ratio of V to **1** or **2** show that the redox reaction is nearly quantitative if the surface coverage is below ~0.5 ML to allow sufficient room for mixing.

High-resolution STM images indicate the formation of 1D metal-ligand polymer chains when V is mixed with either **1** (Fig. 1e, 2a, 2c) or **2** (Fig. 1f, 2b) on the Au(100) surface. The

structures of the metal-organic 1D polymers for each of the two ligands in this study are nearly identical. Each has a morphology that is markedly different from the rectangular 2D islands of pure V (without ligand) on the same surface (Fig. 1d) or from either the 2D domains of metal-free **1** molecules [7] or the mobile and unresolved sub-monolayer phase of metal-free **2** molecules. Zoom-in STM images of the 1D polymers (Fig. 2c) reveal an in-plane rotation of the long molecular axis relative to the chain direction, consistent with the formation of a quasi-square-planar binding pocket around the V centers that consists of two N of tetrazine units and two N of either pyridinyl or pyrimidinyl groups. The repeat distance is 6.5 Å ± 0.4 Å with the molecular axis oriented at a 55 ± 5° angle to the chain direction. Based on the repeat distance within the chain, the molecule orientation, and the known structure of the molecule, the V-N bond length in these structures is determined to be 2-2.5 Å. The **1**-V and **2**-V chains are oriented at a 45 ± 5° angle to the Au reconstruction rows (insets of Figs. 2a and 2b). The Au(100) surface spontaneously reconstructs to a quasi-hexagonal c(26×68) structure with a slight surface rumpling in rows that run in the [011] direction [33, 34]; note that these reconstruction rows slightly affect the contrast variation along the chains in Fig. 2c (compare to model in Fig. 2d). The appearance and spacing of features along the chains are uniform in the STM measurements, which is consistent with all of the molecules in a given chain assuming the same orientation. The redox process is most efficient (less annealing required) if the ligand is deposited first and the metal second, but the opposite deposition order produces the same structure, *i.e.*, addition of either ligand to already-formed V islands yields the same 1D metal-ligand polymer structure.

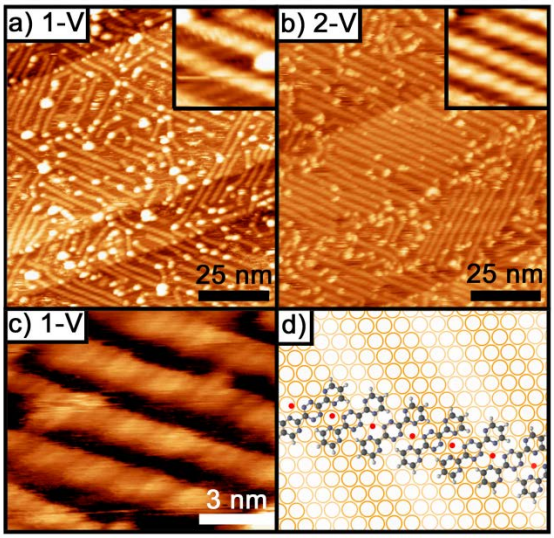

Figure 2. STM images of (a, c) **1**-V and (b) **2**-V chain structures on the reconstructed Au(100) surface. In (a, b), V metal was deposited to the sample first, followed by ligand, and then annealed at 200 °C. In (c) ligand **1** was deposited to the surface first, followed by V, and then annealed at 170 °C. The V:ligand ratio determined from XPS quantification is 1 in each case. The inset images in (a, b) have dimensions of 10 nm × 10 nm. (d) Schematic model of **2**-V chain structure. The **1**-V chain structure is identical.

We have shown that the molecular design of aromatic units pendant to tetrazine can alter the ligand redox character to an extent that is sufficient to achieve different oxidation states in coordinated V atoms. We have thus stabilized single-site V atoms in either a +2 or +3 oxidation

state in 1D metal-ligand assemblies on a surface. The change in the ligand terminal functional groups from pyridinyl to pyrimidinyl functionalization increases the electron withdrawing action from the central tetrazine. The structures of the 1D polymers for either ligand have been shown to be virtually identical by high-resolution STM. In each case the repeat unit consists of a single molecule and single metal. Two tetrazine nitrogen atoms and two pyridinyl (in **1**-V) or pyrimidinyl (in **2**-V) nitrogen atoms are bound to the cationic metals in a near-square-planar coordination geometry. The unbound pyrimidinyl N in **2**-V can accept some of the negative charge attendant to reduction, thus stabilizing the redox change. These experiments demonstrate the possibility of programming the oxidation state of single site transition metals at solid surfaces by coordinating ligand design. This strategy is common in homogeneous catalyst design and is very desirable for developing next-generation heterogeneous catalysts with higher levels of chemical selectivity, particularly for challenging problems in alkane oxidation and functionalization.

2. Metal-Ligand Complexation through Redox Assembly at Surfaces Characterized by Vibrational Spectroscopy

Text and figures in this section are adapted from C. G. Williams, M. Wang, D. Skomski, C. D. Tempas, L. L. Kesmodel, and S. L. Tait, "Metal-Ligand Complexation through Redox Assembly at Surfaces Characterized by Vibrational Spectroscopy," *Journal of Physical Chemistry C*, **121**, 13183-13190 (2017).

In this study we looked at the formation of Pt complexes on Ag(111) and Au(100) using the organic ligand di-pyridyl-tetrazine (DPTZ, Scheme 1). Previous STM and XPS studies have characterized the structure and metal oxidation state for the Pt-DPTZ and V-DPTZ systems on Au(100) [17, 18]. Further insight into the impact of the surface and added electron density in DPTZ will be presented here using vibrational spectroscopy analysis. In addition to Pt-DPTZ complexation on Au(100), the HREELS experiments presented here show the on-surface redox formation of Pt-DPTZ metal-organic coordination complexes on Ag(111) for the first time. We observe DPTZ complexation with Ag adatoms on Ag(111). Ag-DPTZ complexation can also occur as a replacement reaction with Pt-DPTZ on the Ag(111) surface, replacing Pt with Ag atoms. To the best of our knowledge, this is the first observation of the replacement of Pt by Ag within a metal-organic coordination complex in solution or at surfaces. The relative stability of different metals in coordination complexes has been studied previously in solution-based systems [43], including ion exchange processes [44, 45], transmetallation MOF studies [46], and metal-pyridine complexes [43]. However, there are few prior studies of metal replacement reactions at surfaces [47]. Here, we measure differences in HREEL spectra of DPTZ before and after complexation by Ag and Pt to gain insight into the metal-organic complexation process on a metal surface. This work provides an example of vibrational spectroscopy of metal-organic systems at surfaces, which will be important for further chemical analysis of these systems, including potential catalytic and gas adsorption studies.

Ag(111) and Au(100) single crystals were cleaned by cycles of Ar^+ sputtering and thermal annealing. Experiments were conducted in ultra-high vacuum (UHV). DPTZ was vapor deposited from a Knudsen-type evaporator. Pt was vapor deposited by resistive heating of a W filament that was wrapped with fine Pt wire. Post-deposition annealing treatments were done in most experiments, as described below. All HREELS experiments were performed with a double-pass 127° angle cylindrical deflection electron spectrometer (LK Technologies, model LK 2000) operated at an initial beam energy of 5-8 eV and a peak width of 55 ± 10 cm^{-1}. Each spectrum

was normalized by the average intensity of a featureless background region to account for differences in initial beam current.

On-surface redox complexation of DPTZ with Pt on Au(100) has been reported previously using STM and XPS [17]. Upon co-deposition of Pt with DPTZ on Au(100) or on Ag(111), we observe significant HREEL spectra changes consistent with this complexation reaction (Figure 3b). The in-plane pyridine mode and several other in-plane modes shift to higher energy on either Ag(111) or Au(100).

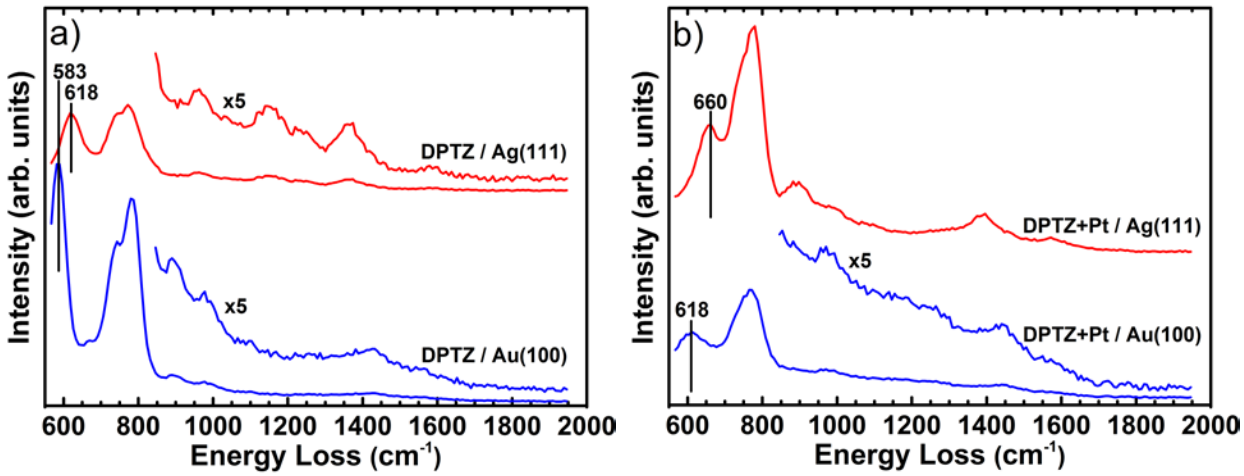

Figure 3. HREELS of the bending mode and in-plane mode regions for (a) DPTZ and (b) DPTZ+Pt on the Ag(111) and Au(100) surfaces. (a) Several differences for in-plane mode positions of non-complexed DPTZ can be observed on the two surfaces, such as the pyridine in-plane mode at a higher energy on Ag(111) (618 cm^{-1}) than on Au(100) (583 cm^{-1}). (b) Several spectral changes after co-deposition of Pt and DPTZ indicate Pt-DPTZ complexation on each surface. The spectrum shown here for Au(100) was recorded after annealing to drive the complexation to completion, but initial complexation is evident before annealing. The Pt-pyridine mode on Ag(111) (660 cm^{-1}) is positioned at a higher energy than on Au(100) (618 cm^{-1}). Multiple differences to the in-plane modes are also observed. The traces have been scaled by the factors indicated in the figure for clarity.

Upon Pt deposition, the out-of-plane deformation mode intensity decreases with respect to the in-plane mode intensity. The ratio of the DPTZ pyridine peak (583 cm^{-1} out-of-plane mode) to in-plane peak height just below 1000 cm^{-1} changes from 3.5 to 2.5 on Ag(111) and from 2.7 to 2.0 on Au(100) (Fig. 3). A C-H stretching mode at 2916 cm^{-1} appears with Pt deposition at room temperature. This peak appearance suggests that some of the aryl C-H are made more aliphatic by the presence of Pt. These relative intensity changes may be partially due to the charge transfer into DPTZ (decrease to out-of-plane modes, increase to in-plane modes, and increase to C-H modes), consistent with previous observations for neutral vs. anionic polyarene species [48, 49]. As far as we can tell, this is one of the first instances of surface-confined redox of a metal and organic species observed through HREELS.

HREEL spectra of DPTZ on Ag(111) at room temperature or after annealing at temperatures up to 80 °C are similar to spectra of DPTZ on Au(100), except for minor spectral differences. However, when DPTZ on Ag(111) is annealed at 110-170 °C (for 90 minutes), significant spectral changes are observed that resemble the spectra for Pt-DPTZ on either Ag(111) or Au(100) more than the spectra for uncomplexed DPTZ on Ag(111) at room temperature (Figure 4), indicating that the DPTZ has complexed with Ag atoms during the annealing. Annealing DPTZ on Au(100) at these temperatures does not produce any notable spectral changes compared to room temperature until DPTZ desorbs from Au(100) at 140 °C, consistent with previous work reporting DPTZ desorption from Au(100) at the same temperature [17]. For HREELS, intensity changes can be due to changes in molecular orientation, but off-specular analysis of the peaks shows that the orientation of the molecule rings remain predominantly parallel with the surface even after the spectral change. It is thus concluded that this annealing caused a redox reaction of the DPTZ with surface Ag atoms creating Ag-DPTZ complexes. DPTZ oxidation of substrate atoms to form Ag-DPTZ complexes on Ag(111) is consistent with the observation above that DPTZ on Ag(111) has a strong pyridine-Ag surface interaction.

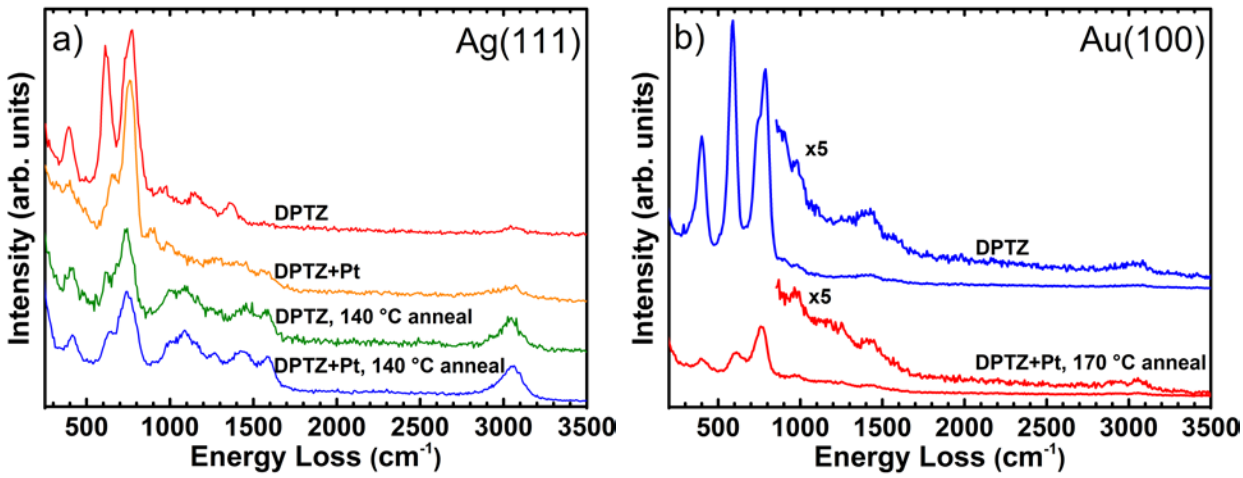

Figure 4. Comparison of HREEL spectra of DPTZ and DPTZ+Pt, before and after annealing at 140-170 °C, on (a) Ag(111) and (b) Au(100). (a) DPTZ on Ag(111) shows a pyridine peak at 618 cm^{-1} (red), but, with Pt co-deposition, that peak shifts to 660 cm^{-1} and in-plane modes also change (orange), indicating Pt complexation with DPTZ. When either DPTZ (green) or DPTZ+Pt (blue) are annealed to 140 °C for 90 minutes, the pyridine peak moves to 640 cm^{-1} and other in-plane peak position align, indicating that both form the same Ag-DPTZ complex, *i.e.*, Ag replaces Pt. (b) On the Au(100) surface, the pyridine mode for DPTZ appears at 583 cm^{-1} (blue) and the molecule begins to desorb with annealing at 140 °C. With Pt co-deposition and annealing to 170 °C, the pyridine mode shifts to 618 cm^{-1}. Note that Pt-DPTZ shows indications of partial complexation after deposition at room temperature before annealing and that complexation with Pt stabilizes DPTZ against thermal desorption.

Annealing Pt-DPTZ complexes on Ag(111) at 80 °C (for 90 minutes) led to HREEL spectral changes similar to Ag-DPTZ on Ag(111), indicating a change in the complex from Pt-DPTZ to Ag-DPTZ. The most notable change upon annealing is a shift of the pyridine out-of-plane deformation from 660 cm^{-1} to 640 cm^{-1}. The direction of this shift is consistent with the difference between Pt and Ag pyridine complexes reported in previous calculations [50]. This shift can also be found in a metal-N bond observed at 194 cm^{-1} for Pt-DPTZ and at 179 cm^{-1} for Ag-DPTZ, albeit this peak is harder to characterize due to the elastic peak background. The vibrational spectrum for Pt-DPTZ on Ag(111) after annealing shows a better match to the spectrum for DPTZ annealed on Ag(111) (forming Ag-DPTZ complexes) than it does to the spectrum for Pt-DPTZ before annealing (Figure 4a).

HREEL spectroscopy was employed to characterize the adsorption and transition metal complexation of DPTZ on Ag(111) and Au(100) surfaces. The surface impacted the complexation behavior after annealing the ligand on each surface; when DPTZ is deposited on Ag(111) and annealed, the ligand is able to capture Ag adatoms to form Ag-DPTZ complexes, but no such reaction occurs on Au(100). Pt co-deposition with DPTZ on Ag(111) or on Au(100) produces Pt-DPTZ immediately after deposition at room temperature. We also observed a replacement reaction by which Pt-DPTZ complexes on Ag(111) converted to Ag-DPTZ complexes upon annealing. The replacement of Pt by Ag has not been reported in any prior metal-organic coordination study at surfaces or in solution. This replacement reaction occurred at a lower temperature than the complexation of neutral DPTZ with Ag adatoms, indicating that the prior redox state facilitated the replacement reaction. Development and understanding of the formation of metal organic complexes is important when trying to design functional surface structures. Here we showed that the surface plays a critical role in the formation of metal organic surface structures and demonstrated the utility of HREELS for studying on-surface redox processes.

3. Dehydrocyclization of Peripheral Alkyl Groups in Porphyrins at Cu(100) and Ag(111) Surfaces

Text and figures in this section adapted from C. G. Williams, M. Wang, D. Skomski, C. D. Tempas, L. L. Kesmodel, and S. L. Tait, "Dehydrocyclization of Peripheral Alkyl Groups in Porphyrins at Cu(100) and Ag(111) Surfaces," *Surface Science*, **653**, 130-137 (2016).

Studies of surface patterning and functionalization by tailored organic molecules often employ relatively inert surfaces, such as Au, Ag, Cu, and graphite. As larger and more complex molecules are developed for surface functionalization, the thermal adsorption stability increases and new surface-catalyzed reaction pathways need to be considered as these may impact short-term and long-term performance of these layers. Here, we study the dehydrocylization of ethyl-functionalized porphyrin molecules on Cu(100) and Ag(111) surfaces upon annealing to 500 - 600 K (Scheme 2).

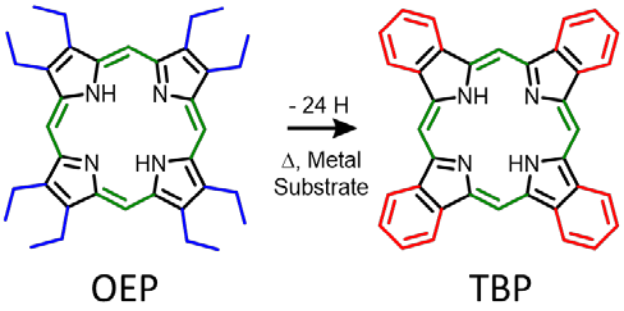

Scheme 2. Dehydrocyclization of octaethylporphyrin (OEP) to tetrabenzoporphyrin (TBP).

OEP and Pt-OEP were deposited at 490 K and TBP at 620 K from a Knudsen-type evaporator. Cu(100) or Ag(111) surfaces were cleaned by cycles of Ar^+ sputtering and thermal annealing. All HREELS experiments were performed with a double-pass 127° angle cylindrical deflection electron spectrometer (LK Technologies, model LK 2000) operated at an initial beam energy of 10 eV and a peak width of 58 ± 6 cm^{-1}. STM imaging and XPS acquisition were conducted at room temperature.

After heating OEP on Cu(100) to 500 K, significant spectral changes are observed compared to before annealing (see Fig. 5). The spectrum matches very well with a previously reported HREELS study of Cu-phthalocyanine (Cu-Pc) and other Pc molecules [51-54]. These changes indicate a chemical transformation of the peripheral ethyl groups to aromatic benzo groups, *i.e.*, a dehydrocyclization (Scheme 2). The temperature of 500 K is consistent with other studies of dehydrogenation of ethyl groups and C-H bond scission on Cu and other surfaces [55, 56]. The dehydrocyclization of OEP on Cu(100) at 500 K (15 minute anneal) (Fig. 5) is higher in temperature than a previous report for the dehydrocyclization of Fe-OEP on Cu(111) at 430 K (60 minute anneal) [56].

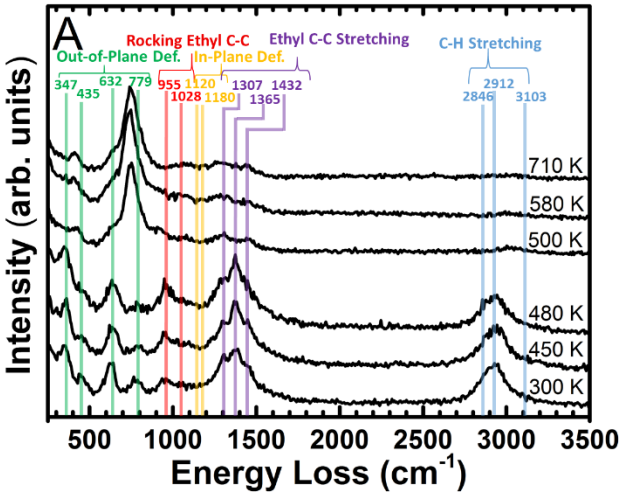

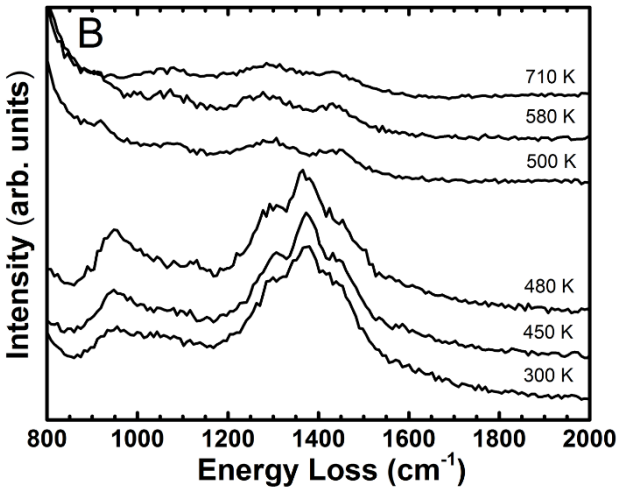

Fig. 5. (A) HREEL spectra of OEP (metallated to Cu-OEP) on Cu(100) after annealing incrementally up to 710 K for 15 minutes at each temperature. Each spectrum was recorded after cooling the sample to room temperature. Major spectroscopic changes after annealing to 500 K include an increase to C-H bending (735 cm^{-1}), decrease to the ethyl rocking and stretching modes (close-up in B, 5× scaling relative to A), and a significant decrease in the C-H region.

Most of the intensity of the C-H stretching feature is lost upon dehydrocyclization. The small remnant of this peak is likely due to hydrogen on the benzo groups (red carbons after dehydrocyclization reaction in Scheme 2) and the four porphyrin methine C-H bonds (green carbon in Scheme 2); these may all be weak HREELS signals because of their orientation parallel to the surface. The C-H position after dehydrocyclization is above 3000 cm^{-1}, *i.e.*, the remaining C-H bonds on the porphyrin core are stronger than the ethyl C-H before dehydrocyclization, as expected [57].

Dehydrocyclization of OEP takes place 100 K higher on the Ag(111) surface (600 K) than on the Cu(100) surface (500 K). It has been demonstrated that porphyrins will self-metallate on the Cu(100) surface at room temperature [58], so we investigated whether the reaction temperature differences were due to metallation of the porphyrin rather than inherent differences in surface reactivity. We found that the dehydrocyclization of Pt-OEP occurs at the same temperature as OEP on Cu(100) and on Ag(111).

STM imaging before (Figs. 6A and 6B) and after (Figs. 6C and 6D) annealing above 600 K shows a significant structural change that also indicates dehydrocyclization. Before annealing OEP molecules are imaged as single lobes on each surface. After annealing above 600 K, each OEP molecule is imaged in STM as a four-lobe structure on either surface. The distance between diagonal lobes is 1.1 nm, consistent with the positions of opposite benzo groups in TBP.

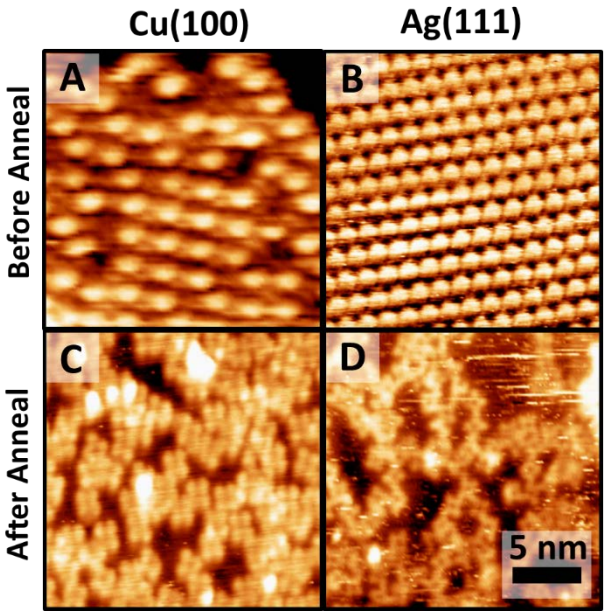

Fig. 6. STM images of OEP (A, C) on Cu(100) and (B, D) on Ag(111) (A, B) before and (C, D) after annealing above 600 K. (A, B) Before dehydrocyclization, OEP appears in STM as a single-lobed feature. (C, D) After annealing above the dehydrocyclization temperature, the OEP has converted to TBP and appears as a four-fold symmetric structure. Scale bar in the lower right applies to all four images. Images were recorded at room temperature (A, B) without annealing or after annealing to (C) 610 K or (D) 710 K. STM bias 1.0 – 1.2 V, setpoint current 0.2 – 0.4 nA.

It is likely that the dehydrocyclization mechanism here is similar to that derived for hexenes on a Cu_3Pt surface [59, 60]. The first dehydrogenation on the ethyl group is likely at the more acidic allylic α carbon hydrogen. The subsequent dehydrogenation of the β carbon forms the vinyl species, which then undergoes a 6π pericyclic rearrangement, followed by further dehydrogenation to form the benzo group (Scheme 3). Normally, alkane/alkene C-C bond formation is significantly slower than further dehydrogenation [61], but the positioning of the two ethyl groups in neighboring positions on the porphyrin ring may favor cyclization over further dehydrogenation.

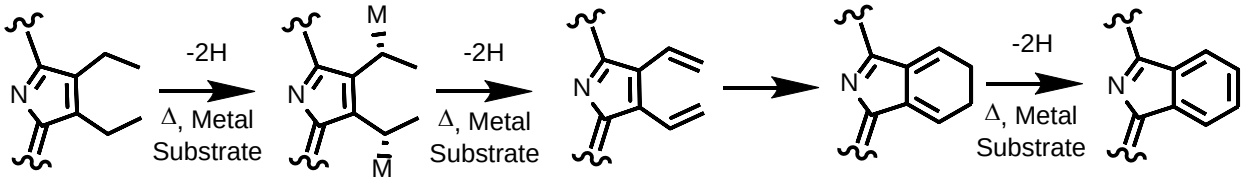

Scheme 3. Proposed mechanism for the dehydrocyclization of ethyl groups on OEP.

HREEL spectroscopy and STM provide evidence for the dehydrocyclization of the peripheral ethyl units of OEP on Cu(100) and Ag(111) surfaces. While smaller alkane

functionalized species would desorb before this reaction takes place, OEP has sufficient stability against thermal desorption for the reaction at 500 and 610 K on Cu(100) and Ag(111), respectively. The dehydrocyclized product then undergoes an additional dehydrogenation step of its benzo aryl hydrogens. This aryl dehydrogenation was also found to occur when TBP is deposited and annealed to 480 K or 500 K on Cu(100) or Ag(111), respectively. The dehydrocyclized OEP and aryl dehydrogenated TBP have very similar spectral features and both are likely forming surface bonds. Metallation of the porphyrin ring, tested by deposition of Pt-OEP or self-metallation on the Cu surface, did not have any effect on the dehydrocyclization temperature. Reaction steps such as these are important considerations in the ongoing development of more sophisticated functional organic architectures at surfaces and in advancing our understanding of surface catalysis.

List of publications in which DOE support is acknowledged

1. C. G. Williams, M. Wang, D. Skomski, C. D. Tempas, L. L. Kesmodel, and S. L. Tait, "Metal-Ligand Complexation through Redox Assembly at Surfaces Characterized by Vibrational Spectroscopy," *Journal of Physical Chemistry C*, **121**, 13183-13190 (2017). DOI: 10.1021/acs.jpcc.7b02809
2. C. D. Tempas, D. Skomski, and S. L. Tait, "Lifting of the Au(100) Surface Reconstruction by Pt, Cr, Fe, and Cu Adsorption," *Surface Science*, **654**, 33-38 (2016). DOI: 10.1016/j.susc.2016.07.012
3. C. G. Williams, M. Wang, D. Skomski, C. D. Tempas, L. L. Kesmodel, and S. L. Tait, "Dehydrocyclization of Peripheral Alkyl Groups in Porphyrins at Cu(100) and Ag(111) Surfaces," *Surface Science*, **653**, 130-137 (2016). DOI: 10.1016/j.susc.2016.06.013
4. D. Skomski, C. D. Tempas, B. J. Cook, A. V. Polezhaev, K. A. Smith, K. G. Caulton, and S. L. Tait, "Two and Three Electron Oxidation of Single-site Vanadium Centers at Surfaces by Ligand Design," *Journal of the American Chemical Society, **137**, 7898-7902* (2015). DOI: 10.1021/jacs.5b03706
5. D. Skomski, C. D. Tempas, G. S. Bukowski, K. A. Smith, and S. L. Tait, "Redox-Active On-Surface Polymerization of Single-Site Divalent Cations from Pure Metals by a Ketone-Functionalized Phenanthroline," *Journal of Chemical Physics*, **142**, *101913* (2015). DOI: 10.1063/1.4906894
6. D. Skomski, J. Jo, C. D. Tempas, S. Kim, D. Lee, and S. L. Tait, "High-Fidelity Self-Assembly of Crystalline and Parallel-Oriented Organic Thin Films by π–π Stacking from a Metal Surface," *Langmuir, **30**, 10050-10056* (2014). DOI: 10.1021/la502288v
7. D. Skomski, C. D. Tempas, K. A. Smith, and S. L. Tait, "Redox-Active On-Surface Assembly of Metal-Organic Chains with Single-Site Pt(II)," *Journal of the American Chemical Society, **136**, 9862-9865* (2014). DOI: 10.1021/ja504850f
8. D. Skomski and S. L. Tait, "Interfacial Organic Layers as Templates for Crystalline Organic Films with Carboxyl and Thiophene Functionalization," *Journal of Physical Chemistry C*, **118**, 1594-1601 (2014). DOI: 10.1021/jp409799f

References

[1] J. Boscoboinik, J. Kestell, M. Garvey, M. Weinert, W.T. Tysoe, Creation of Low-Coordination Gold Sites on Au(111) Surface by 1,4-phenylene Diisocyanide Adsorption, Top. Catal., 54 (2011) 20-25.
[2] G.L. Simard, J.F. Steger, R.J. Arnott, L.A. Siegel, Vanadium Oxides as Oxidation Catalysts, Industrial and Engineering Chemistry, 47 (1955) 1424-1430.
[3] W. Weng, M. Davies, G. Whiting, B. Solsona, C.J. Kiely, A.F. Carley, S.H. Taylor, Niobium phosphates as new highly selective catalysts for the oxidative dehydrogenation of ethane, Phys. Chem. Chem. Phys., 13 (2011) 17395-17404.
[4] J.M. Gottfried, K. Flechtner, A. Kretschmann, T. Lukasczyk, H.P. Steinrück, Direct synthesis of a metalloporphyrin complex on a surface, J. Am. Chem. Soc., 128 (2006) 5644-5645.
[5] Y. Bai, F. Buchner, M.T. Wendahl, I. Kellner, A. Bayer, H.P. Steinrück, H. Marbach, J.M. Gottfried, Direct metalation of a phthalocyanine monolayer on Ag(111) with coadsorbed iron atoms, J. Phys. Chem. C, 112 (2008) 6087-6092.
[6] S.L. Tait, Y. Wang, G. Costantini, N. Lin, A. Baraldi, F. Esch, L. Petaccia, S. Lizzit, K. Kern, Metal-organic coordination interactions in Fe-Terephthalic acid networks on Cu(100), J. Am. Chem. Soc., 130 (2008) 2108-2113.
[7] D. Skomski, C.D. Tempas, K.A. Smith, S.L. Tait, Redox-active On-surface Assembly of Metal-organic Chains with Single-site Pt(II), J. Am. Chem. Soc., 136 (2014) 9862-9865.
[8] D. Skomski, C.D. Tempas, G.S. Bukowski, K.A. Smith, S.L. Tait, Redox-active on-surface polymerization of single-site divalent cations from pure metals by a ketone-functionalized phenanthroline, J. Chem. Phys., 142 (2015) 101913.
[9] M. Valden, X. Lai, D.W. Goodman, Onset of catalytic activity of gold clusters on titania with the appearance of nonmetallic properties, Science, 281 (1998) 1647-1650.
[10] B. Hvolbæk, T.V. Janssens, B.S. Clausen, H. Falsig, C.H. Christensen, J.K. Nørskov, Catalytic activity of Au nanoparticles, Nano Today, 2 (2007) 14-18.
[11] M. Haruta, M. Daté, Advances in the catalysis of Au nanoparticles, Applied Catalysis A: General, 222 (2001) 427-437.
[12] R. Narayanan, M.A. El-Sayed, Shape-dependent catalytic activity of platinum nanoparticles in colloidal solution, Nano Lett., 4 (2004) 1343-1348.
[13] Q. Fu, H. Saltsburg, M. Flytzani-Stephanopoulos, Active nonmetallic Au and Pt species on ceria-based water-gas shift catalysts, Science, 301 (2003) 935-938.
[14] A. Corma, H. Garcia, Supported gold nanoparticles as catalysts for organic reactions, Chem. Soc. Rev., 37 (2008) 2096-2126.
[15] A.S.K. Hashmi, Gold-catalyzed organic reactions, Chem. Rev., 107 (2007) 3180-3211.
[16] J. Boscoboinik, J. Kestell, M. Garvey, M. Weinert, W. Tysoe, Creation of Low-Coordination Gold Sites on Au(111) Surface by 1,4-phenylene Diisocyanide Adsorption, Top. Catal., 54 (2011) 20-25.
[17] D. Skomski, C.D. Tempas, K.A. Smith, S.L. Tait, Redox-Active On-Surface Assembly of Metal–Organic Chains with Single-Site Pt(II), J. Am. Chem. Soc., 136 (2014) 9862-9865.
[18] D. Skomski, C.D. Tempas, B.J. Cook, A.V. Polezhaev, K.A. Smith, K.G. Caulton, S.L. Tait, Two- and Three-Electron Oxidation of Single-Site Vanadium Centers at Surfaces by Ligand Design, J. Am. Chem. Soc., 137 (2015) 7898-7902.
[19] O. Shekhah, J. Liu, R. Fischer, C. Wöll, MOF thin films: existing and future applications, Chem. Soc. Rev., 40 (2011) 1081-1106.
[20] J.-L. Zhuang, A. Terfort, C. Wöll, Formation of oriented and patterned films of metal–organic frameworks by liquid phase epitaxy: A review, Coordin Chem Rev, 307, Part 2 (2016) 391-424.
[21] L. Heinke, M. Tu, S. Wannapaiboon, R.A. Fischer, C. Wöll, Surface-mounted metal-organic frameworks for applications in sensing and separation, Microporous and Mesoporous Materials, 216 (2015) 200-215.

[22] B. Liu, O. Shekhah, H.K. Arslan, J. Liu, C. Wöll, R.A. Fischer, Enantiopure Metal–Organic Framework Thin Films: Oriented SURMOF Growth and Enantioselective Adsorption, Angew. Chem. Int. Ed., 51 (2012) 807-810.
[23] Y. Li, J. Xiao, T.E. Shubina, M. Chen, Z. Shi, M. Schmid, H.-P. Steinrück, J.M. Gottfried, N. Lin, Coordination and metalation bifunctionality of Cu with 5, 10, 15, 20-tetra (4-pyridyl) porphyrin: toward a mixed-valence two-dimensional coordination network, J. Am. Chem. Soc., 134 (2012) 6401-6408.
[24] L. Dong, Z.A. Gao, N. Lin, Self-assembly of metal–organic coordination structures on surfaces, Progress in Surface Science, 91 (2016) 101-135.
[25] T. Lin, Q. Wu, J. Liu, Z. Shi, P.N. Liu, N. Lin, Thermodynamic versus kinetic control in self-assembly of zero-, one-, quasi-two-, and two-dimensional metal-organic coordination structures, J. Chem. Phys., 142 (2015) 101909.
[26] W. Kaim, The coordination chemistry of 1,2,4,5-tetrazines, Coordin. Chem. Rev., 230 (2002) 127-139.
[27] I.W.C.E. Arends, R.A. Sheldon, M. Wallau, U. Schuchardt, Oxidative transformations of organic compounds mediated by redox molecular sieves, Angew. Chem., Int. Ed., 36 (1997) 1144-1163.
[28] A.V. Ramaswamy, S. Sivasanker, Selective Oxidation Reactions over Titanium and Vanadium Metallosilicate Molecular-Sieves, Catal. Lett., 22 (1993) 239-249.
[29] K.C. Gupta, A.K. Sutar, Catalytic activities of Schiff base transition metal complexes, Coord. Chem. Rev., 252 (2008) 1420-1450.
[30] G.W. Coates, P.D. Hustad, S. Reinartz, Catalysts for the Living Insertion Polymerization of Alkenes: Access to New Polyolefin Architectures Using Ziegler–Natta Chemistry, Angew. Chem. Int. Ed., 41 (2002) 2236-2257.
[31] T. Hirao, Vanadium: Organometallic Chemistry, in: Encyclopedia of Inorganic Chemistry, John Wiley & Sons, Ltd, 2006.
[32] G. Silversmit, D. Depla, H. Poelman, G.B. Marin, R. De Gryse, Determination of the V2p XPS binding energies for different vanadium oxidation states (V5+ to V0+), J. Electron Spectrosc. Relat. Phenom., 135 (2004) 167-175.
[33] M.A. Vanhove, R.J. Koestner, P.C. Stair, J.P. Bibérian, L.L. Kesmodel, I. Bartoš, G.A. Somorjai, The Surface Reconstructions of the (100) Crystal Faces of Iridium, Platinum and Gold 1. Experimental-Observations and Possible Structural Models, Surf. Sci., 103 (1981) 189-217.
[34] M.A. Vanhove, R.J. Koestner, P.C. Stair, J.P. Biberian, L.L. Kesmodel, I. Bartos, G.A. Somorjai, The Surface Reconstructions of the (100) Crystal Faces of Iridium, Platinum and Gold .2. Structural Determination by Leed Intensity Analysis, Surf. Sci., 103 (1981) 218-238.
[35] W. Kaim, J. Fees, The New Tetrafunctional Pi-Acceptor Ligand 3,6-Bis(2'-Pyrimidyl)-1,2,4,5-Tetrazine (Bmtz) - Diruthenium Complexes of Bmtz and of Its 1,4-Dihydro Form, Z. Naturforsch. B, 50 (1995) 123-127.
[36] J. Kasperkiewicz, J.A. Kovacich, D. Lichtman, Xps Studies of Vanadium and Vanadium-Oxides, J. Electron Spectrosc. Relat. Phenom., 32 (1983) 123-132.
[37] D.P. Woodruff, T.A. Delchar, Modern Techniques of Surface Science, 2nd ed., Cambridge University Press, Cambridge ; New York, 1994.
[38] K. Eguchi, T. Nakagawa, Y. Takagi, T. Yokoyama, Direct Synthesis of Vanadium Phthalocyanine and Its Electronic and Magnetic States in Monolayers and Multilayers on Ag(111), J. Phys. Chem. C, 119 (2015) 9805-9815.
[39] J.F. Moulder, J. Chastain, Handbook of X-ray Photoelectron Spectroscopy: A Reference Book of Standard Spectra for Identification and Interpretation of XPS data, Physical Electronics Division, Perkin-Elmer Corp., Eden Prairie, Minn., 1992.
[40] T.K.A. Hoang, M.I. Webb, H.V. Mai, A. Hamaed, C.J. Walsby, M. Trudeau, D.M. Antonelli, Design and Synthesis of Vanadium Hydrazide Gels for Kubas-Type Hydrogen Adsorption: A New Class of Hydrogen Storage Materials, J. Am. Chem. Soc., 132 (2010) 11792-11798.

[41] in, XPS reference data for the V(I) and V(II) charge states are rare. In vanadium oxides, the feature at 513.7 eV (which matches the value for 1-V) is thought to correspond to vanadium(II) since a pure vanadium(I) oxide structure does not exist.
[42] The Au surface likely plays some role in affecting the final charge distribution of the system. Detailed theoretical studies, which are beyond the scope of this work, will be needed to fully address these questions. However, we note that the extent of redox observed spectroscopically here can be fully rationalized by in-plane charge transfer and known redox potentials of the employed ligands and metals. Indeed, in our studies so far of these and similar on-surface redox processes (Refs. 7-8), we have not yet observed significant deviations from solution-based redox behavior due to the surfaces, but perhaps other surfaces would play a more active role.
[43] H. Irving, R. Williams, 637. The stability of transition-metal complexes, Journal of the Chemical Society (Resumed), (1953) 3192-3210.
[44] V.J. Inglezakis, M.D. Loizidou, H.P. Grigoropoulou, Ion exchange of Pb2+, Cu2+, Fe3+, and Cr3+ on natural clinoptilolite: selectivity determination and influence of acidity on metal uptake, J. Colloid Interface Sci., 261 (2003) 49-54.
[45] J.N. Armor, Metal-exchanged zeolites as catalysts1, Microporous and Mesoporous Materials, 22 (1998) 451-456.
[46] M. Lalonde, W. Bury, O. Karagiaridi, Z. Brown, J.T. Hupp, O.K. Farha, Transmetalation: Routes to Metal Exchange Within Metal–Organic Frameworks, J. Mater. Chem. A, 1 (2013).
[47] J.M. Gottfried, Surface chemistry of porphyrins and phthalocyanines, Surf. Sci. Rep., 70 (2015) 259-379.
[48] S.R. Langhoff, Theoretical infrared spectra for polycyclic aromatic hydrocarbon neutrals, cations, and anions, J. Phys. Chem., 100 (1996) 2819-2841.
[49] J. Szczepanski, C. Wehlburg, M. Vala, Vibrational and electronic spectra of matrix-isolated pentacene cations and anions, Chemical physics letters, 232 (1995) 221-228.
[50] D.-Y. Wu, B. Ren, Y.-X. Jiang, X. Xu, Z.-Q. Tian, Density Functional Study and Normal-Mode Analysis of the Bindings and Vibrational Frequency Shifts of the Pyridine−M (M = Cu, Ag, Au, Cu+, Ag+, Au+, and Pt) Complexes, J. Phys. Chem. A, 106 (2002) 9042-9052.
[51] J.M. Auerhammer, M. Knupfer, H. Peisert, J. Fink, The Copper Phthalocyanine/Au(100) Interface Studied using High Resolution Electron Energy-Loss Spectroscopy, Surf. Sci., 506 (2002) 6.
[52] E. Salomon, T. Angot, N. Papageorgiou, J.M. Layet, Self-Assembled Monolayer of Tin-Phthalocyanine on InSb(001)-(4×2)/c(8×2), Surf. Sci., 596 (2005) 74-81.
[53] F. Roth, A. König, R. Kraus, M. Grobosch, T. Kroll, M. Knupfer, Probing the Molecular Orbitals of FePc Near the Chemical Potential using Electron Energy-Loss Spectroscopy, Euro. Phys. J. B, 74 (2010) 339-344.
[54] P. Amsalem, L. Giovanelli, J. Themlin, T. Angot, Electronic and vibrational properties at the ZnPc/Ag(110) interface, Phys. Rev. B, 79 (2009) 235426.
[55] S. Haq, F. Hanke, M.S. Dyer, M. Persson, P. Iavicoli, D.B. Amabilino, R. Raval, Clean Coupling of Unfunctionalized Porphyrins at Surfaces to give Highly Oriented Organometallic Oligomers, J. Am. Chem. Soc., 133 (2011) 12031-12039.
[56] D. van Vörden, M. Lange, M. Schmuck, J. Schaffert, M.C. Cottin, C.A. Bobisch, R. Möller, Communication: Substrate Induced Dehydrogenation: Transformation of Octa-ethyl-porphyrin into Tetra-benzo-porphyrin, J. Chem. Phys., 138 (2013) 211102.
[57] H. Ogoshi, N. Masai, Z. Yoshida, J. Takemoto, K. Nakamoto, The Infrared Sprectra of Metallooctaehtyl Porphyrins, Bull. Chem. Soc. Jpn., 44 (1971) 3.
[58] R. González-Moreno, C. Sánchez-Sánchez, M. Trelka, R. Otero, A. Cossaro, A. Verdini, L. Floreano, M. Ruiz-Bermejo, A. García-Lekue, J.A. Martín-Gago, C. Rogero, Following the Metalation Process of Protoporphyrin IX with Metal Substrate Atoms at Room Temperature, J. Phys. Chem. C, 115 (2011) 6849-6854.
[59] A.V. Teplyakov, B.E. Bent, Mechanism of Dehydrocyclization of 1-Hexene to Benzene on Cu3Pt(111), J. Phys. Chem. B, 101 (1997) 9052-9059.

[60] A.V. Teplyakov, A.B. Gurevich, E.R. Garland, B.E. Bent, J.G. Chen, Mechanism of Dehydrocyclization of 1-Hexene to Benzene on Cu3Pt(111): Identification of 1,3,5-Hexatriene as Reaction Intermediate, Langmuir, 14 (1998) 1337-1344.
[61] A. Paul, M.X. Yang, B.E. Bent, Disproportionation and Coupling Reactions of Alkyl Iodides on a Au(111) Surface, Surf. Sci., 297 (1993) 327-344.